

Article

Evolution and Prediction of the Coupling Coordination Degree of Production–Living–Ecological Space Based on Land Use Dynamics in the Daqing River Basin, China

Qing Liu, Dongdong Yang * and Lei Cao

School of Architecture, Tianjin University, Tianjin 300072, China

* Correspondence: dd.yang@tju.edu.cn

Abstract: Located in China's Beijing–Tianjin–Hebei region, the Daqing River Basin has a high economic development level. The natural and social conditions within the basin vary greatly, and the spatial configuration of the Production–Living–Ecological Space (PLES) between different sub-regions is unbalanced, with problems and contradictions in the functions of PLES becoming increasingly prominent. This study constructs a PLES classification system for the Daqing River Basin based on multi-period land use data, simulates the future land use evolution of the basin using the Patch-Generating Land Use Simulation (PLUS) model, calculates the coupling degree (CD) coupling coordination degree (CCD) of PLES from 1992 to 2020, and, under the natural trend development scenario (NT), cropland preservation development scenario (CP), and ecological preservation development scenario (EP) of 2030, quantitatively analyses the historical evolution and future direction of the three-life spatial. The results show that: (1) From 1992 to 2020, the area of living space in the Daqing River Basin has increased significantly, while the area of production space and ecological space has decreased significantly. Compared to NT, CP is beneficial to the maintenance of production space, while the EP is beneficial to the maintenance of ecological space. (2) Globally, the CD and the CCD of PLES in the Daqing River Basin show an increasing trend from 1992 to 2010 and a decreasing trend from 2010 to 2020. In 2030, the CD and the CCD of PLES of the three development scenarios decrease significantly compared to 2020; however, the decrease in CP is slight. (3) By region, from 1992 to 2020, the CCD of PLES in the western and eastern parts of the Daqing River Basin increases relatively more, while the central part increases slightly. Compared to 2020, the CCD of PLES in the central part of the Daqing River Basin is predicted to decrease significantly under NT and EP in 2030, while the decrease is slightly less under CP. In all three scenarios, there are some areas where the CCD of PLES increases in the western areas. This study highlights the internal variability of the spatial evolution of PLES in the basin and focuses on the impact of different future development scenarios on the spatial changes of PLES, which can offer an enlightenment for high-quality development and sustainable territorial spatial planning in the Daqing River Basin.

Keywords: production–living–ecological space (PLES); coupling coordination degree; land use; multi-scenarios prediction; basin governance; the Daqing River Basin



Citation: Liu, Q.; Yang, D.; Cao, L. Evolution and Prediction of the Coupling Coordination Degree of Production–Living–Ecological Space Based on Land Use Dynamics in the Daqing River Basin, China. *Sustainability* **2022**, *14*, 10864. <https://doi.org/10.3390/su141710864>

Academic Editor: Brian Deal

Received: 20 July 2022

Accepted: 23 August 2022

Published: 31 August 2022

Publisher's Note: MDPI stays neutral with regard to jurisdictional claims in published maps and institutional affiliations.



Copyright: © 2022 by the authors. Licensee MDPI, Basel, Switzerland. This article is an open access article distributed under the terms and conditions of the Creative Commons Attribution (CC BY) license (<https://creativecommons.org/licenses/by/4.0/>).

1. Introduction

Human social development has led to huge changes in earth surface space, with the transfer of forest, grassland, and wetland in their original state to cropland, production land, and residential land being an extremely distinctive feature [1]. Since the Reform and Opening Up in 1978, China's rapid socio-economic development has greatly accelerated the rate of conversions between land use types in China, thus dramatically changing the quantity and distribution of each type of land use [2,3]. As a result of the different patterns of socio-economic development, the main land use types have been converted differently in different regions. In some regions, the sprawl of built-up land and cropland has come

at the expense of shrinking forest and wetland, such as in the Amazon basin of South America [4–6] and in Africa [7,8]. In other regions, especially those with relatively mature farming economies, such as northern China [9,10] and the various plain regions of southern China [11], the sprawl of built-up land has been at the expense of shrinking cropland, although policies related to cropland preservation have proliferated, which, in essence, has resulted in a continued shrinkage of cropland.

Land use change has far-reaching consequences for the state of the environment and for sustainable development [12–16]. For the development of human society, living space, production space, and ecological space (PLES) provide the basic conditions for human activities and are essential for human survival, and all three are indispensable [17,18]. Along with the rapid sprawl of built-up land, the relationship between PLES has become seriously imbalanced in China [19,20]. Thus, it is important to understand the historical evolution of PLES and to explore the direction of PLES in future development scenarios in order to boost the sustainable development of human society.

In recent years, the idea of basin-based development as a boundary has gradually gained importance, and land use is the substrate for socio-economic development in a basin [21–23]. The introduction of the Promotion of Ecological Conservation and High-Quality Development of the Upper Reaches of the Yellow River [24] has further reversed the shackles of the traditional administrative boundary as a development unit, and the need to understand the spatial evolution patterns of PLES within the framework of basins has become increasingly strong across China for the sake of sustainable economic and social development. As a result, optimising the quantitative and distributional patterns of land use in basins and promoting the coordination of PLES within basins are key issues at hand.

The Daqing River Basin is located in the economically developed Beijing–Tianjin–Hebei region of northern China, with extremely high levels of socio-economic activity and population density [25]. Compared to most other regions of China, the economy of the Daqing River Basin developed earlier and at a higher level of economic development [26]. Meanwhile, the degree of development within the Daqing River Basin is uneven. The eastern part of the basin corresponds spatially to the city of Tianjin, which has a supreme level of socio-economic development and the highest population density. The central part corresponds to the city of Baoding in Hebei province, with a very high level of agricultural development and dense administrative units. The western part is mountainous, with a relatively low level of economic development and a low level of alteration of the ground cover type by human activity [27,28]. For such a highly socio-economically developed and heterogeneous basin, it is essential to explore the evolution of its PLES to better understand the effects of economic development on the regional environment. Meanwhile, as economic and social development continues, it is also important to explore how the future spatial evolution of PLES in the Daqing River Basin will change, as this directly determines the form of the spatial carrier on which human society will be based, and is closely related to human well-being.

Some studies have focused on the pattern and evolution of PLES, and these studies can be divided into two categories. One category mainly explores the scale quantity of PLES and its evolution. Yingxian Deng et al. analysed the PLES change and its influencing factors in Guangdong, China, in the context of urbanization [29]. Geying Jiao et al. explored the changes in the spatial distribution pattern of PLES in Wuyuan County, Jiangxi Province, based on the county scale [30]. Kai Li et al. analysed dynamics of the PLES from 2000 to 2020 in the Yangtze River Delta Urban Agglomeration, and found that production space is easily occupied by living space [31]. Yan Zou et al. explored the spatial distribution pattern and spatio-temporal evolution of PLES in Xuzhou City, China, based on the municipal scale [32]. Another category further explored the relationship among production space, living space, and ecological space with the help of two types of indicators: coupling degree (CD) and coupling coordination degree (CCD). Jiansu Li et al. took the Yellow River Basin as the study area and analysed the CD and CCD of PLES at two points in time, 1995 and 2015 [33]. Yuanyuan Yang et al. analysed the evolution of the CCD of PLES in

the Beijing–Tianjin–Hebei region of China between 2000 and 2015 [34]. Lanyi Wei et al. analysed the evolutionary features of the CD of the PLES from 1998 to 2018 in Jilin Province, China [35]. Cheng Wang et al. analysed the CCD of PLES in rural areas of Chongqing [36]. Qiang Li et al. analysed the CCD of PLES in the Fen River Basin of Shanxi Province, China, from 2006 to 2018 [37]. Summarising the existing studies, on the one hand, the time course analysed in these studies is relatively short, generally 10 to 15 years, and, due to the limited duration, the CD and CCD always show a monotonous increase or decrease. It is unclear how CD and CCD change over a long historical period in a developed area of China such as the Daqing River Basin. On the other hand, although some studies have also focused on the future evolution of PLES [38], how the CD and CCD of PLES will change in the future is still unclear.

A variety of land use simulation models exist, most of which predict the amount of land use with linear or non-linear algorithms and then simulate the spatial distribution of land use with a cellular automaton (CA) model. With the popularisation of deep learning techniques, some land use simulation models incorporating deep learning techniques have emerged, such as the future land use simulation (FLUS) model [39] and patch-generating land use simulation (PLUS) model [40]. Among them, the PLUS model has relatively higher simulation accuracy, and many studies have adopted this model for land use simulation [40]. At the provincial scale, Qing Liu et al. used the PLUS model to simulate land use on Hainan Island in multiple scenarios [11]. At the urban cluster scale, Shihe Zhang et al. used the PLUS model to predict land use in the delta region of Fujian Province, China [41]. At the municipal scale, Ziyao Wang et al. used PLUS to simulate land use in Bortala, Xinjiang [42]. In a study area with watershed boundaries, Yongjun Du et al. used PLUS to simulate land use in the Manas River Basin in multiple scenarios [43]. These studies confirm the applicability of the PLUS model in land use simulation.

Comparing the socio-economic characteristics of the Daqing River Basin with the inadequacy of PLES research progress, we found that the Daqing River Basin is a region with research potential. Through an integration of long time series land use change analysis and multi-scenario land use simulations, we aim to investigate the following three questions: (1) What are the features of the change in PLES of the Daqing River Basin over a long-term evolution? (2) What are the changes in the CD and CCD of PLES, whether decreasing or increasing, or lacking monotonicity? (3) How will PLES of the river basin change under different development scenarios in the future? Which development scenario is more conducive to maintaining or slowing down the deterioration of the basin's PLES? By exploring the above questions, our study can help deepen the understanding of the evolution of the basin's PLES and offer solutions for the formulation of sustainable development policies and the implementation of related land use plans.

This study is divided into five sections. In addition to the introduction in this section, Section 2 describes the study area and the data and methods used in this study; Section 3 states the results obtained; Section 4 offers a discussion; and Section 5 presents conclusions.

2. Data Sources and Research Methods

2.1. Study Area

The Daqing River Basin is located in northern China, between $113^{\circ}50'$ – $118^{\circ}00'$ E and $38^{\circ}50'$ – $40^{\circ}10'$ N, with an area of approximately 45,300 km² (Figure 1). The main river of this basin is the Daqing River, and the main tributaries include the Juma River, the Baigou River, the Tang River, and the Zhulong River. The altitude of the basin varies significantly, with the plateau in the west being at an average altitude of more than 1000 m and the North China Plain in the east at an average altitude of less than 50 m. The Daqing River Basin is in a Monsoon Climate of Medium Latitudes area, with high temperatures and rain in summer and cold and dry winters, with annual precipitation of 400–800 mm. The Daqing River Basin covers 66 county level administrative units in Hebei Province, two municipalities directly under the central government (Tianjin and Beijing), and Shanxi Province, with the Tianjin and Baoding downtown areas being located completely within

the basin. The Daqing River basin is socially and economically developed and densely populated; however, the regional development is highly uneven. Tianjin is the economic centre and an important shipping centre in northern China, and Baoding is one of the central cities in the Beijing–Tianjin–Hebei region, forming an economically developed cluster within the basin, while the western mountainous regions are relatively backward in terms of economic development. Considering the heterogeneity of the Daqinghe River Basin at varied aspects, it can be a well-fitted area for exploring our proposed questions. In addition, the central part of the Daqing River Basin is a considerable grain-producing region in China, with wheat and sorghum fields being the main types of cultivation [44,45].

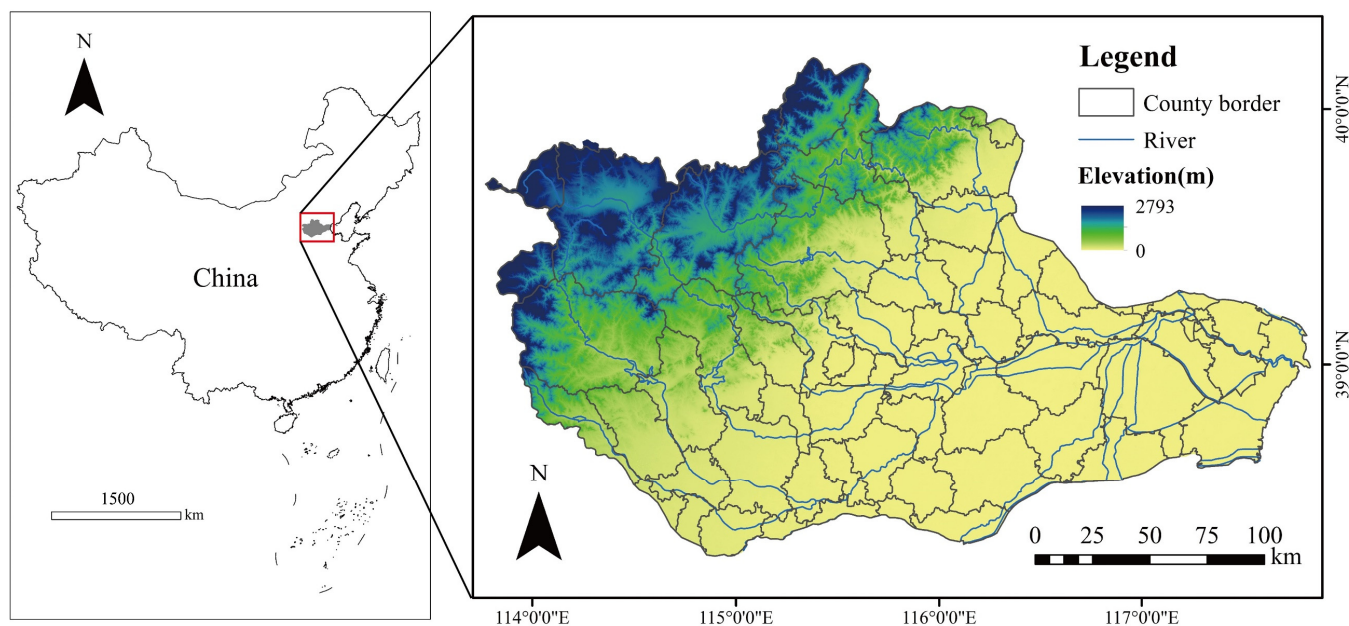


Figure 1. The brief geographical information of the Daqing River Basin.

2.2. Data Sources

Data from varied sources were used in this study (Table 1). We adopted land use data from the European Space Agency’s (ESA) Climate Change Initiative (CCI), which covers the period from 1992 to 2020. Given the large size of the study area, the fact that land use change analysis is one of the focuses of this study and the fact that this dataset is more than 90% accurate, we ultimately decided to use this dataset. This dataset covers 28 years, and it is better than other higher resolution datasets that span a shorter period of time in helping to understand the PLES evolution process. Multi-year average temperature data and multi-year average precipitation data are from the National Meteorological Information Center. Although the climate data up to 2020 can be obtained, since the land use simulation method mentioned below involves training and verification, we selected the climate data from 2010 to 2020 close to the training year for the purpose of improving the training accuracy. Population distribution data, GDP per unit area data, railway network, national road, provincial road, municipality directly under the central government (Tianjin) point, city downtown point, county downtown point, settlement point, and river network data are from the National Earth System Science Data Center <http://www.geodata.cn/> (accessed on 19 July 2022). Digital elevation model (DEM) data are from the United States Geological Survey (USGS). For these social-related land use change drivers, we finally used the data of 2015 to achieve better model training performance. Based on the above raw data, combined with the objective status in the Daqing River Basin and examples of previous studies, and in accordance with the format requirements of the PLUS model for land use change driver data, we produced 15 types of maps of land use change drivers using ArcGIS 10.8.1 (ESRI, USA), including GDP per unit area, population density, distance to Tianjin downtown, distance to cities’ downtowns, distance to counties’ downtowns, distance to settlements,

distance to railways, distance to national roads, distance to provincial roads, distance to rivers, multi-year average precipitation, multi-year average temperature, elevation, slope, and aspect. These above maps characterise the spatial distribution of the drivers of land use evolution in the Daqing River Basin at both the natural and social levels [40] (Figure 2).

Table 1. Data sources and formats of this study.

Data	Data Attribute	Years	Format/Resolution	Sources
LULC	Land use and land cover	1992–2020	Raster/300 m	https://www.esa-landcover-cci.org (accessed on 19 July 2022).
Meteorology	Temperature	2010–2015	Raster/1000 m	https://data.cma.cn (accessed on 19 July 2022).
	Precipitation	2010–2015	Raster/1000 m	https://data.cma.cn (accessed on 19 July 2022).
Geography	DEM	2000	Raster/30 m	https://earthexplorer.usgs.gov (accessed on 19 July 2022).
	River network	2015	Shapefile	http://www.geodata.cn (accessed on 19 July 2022).
Social economy	Population	2015	Shapefile	http://www.geodata.cn (accessed on 19 July 2022).
	GDP			
	Railway network			
	National road			
	Provincial road			
	Municipality directly under the central government point			
	City point			
County point				
Settlement point				

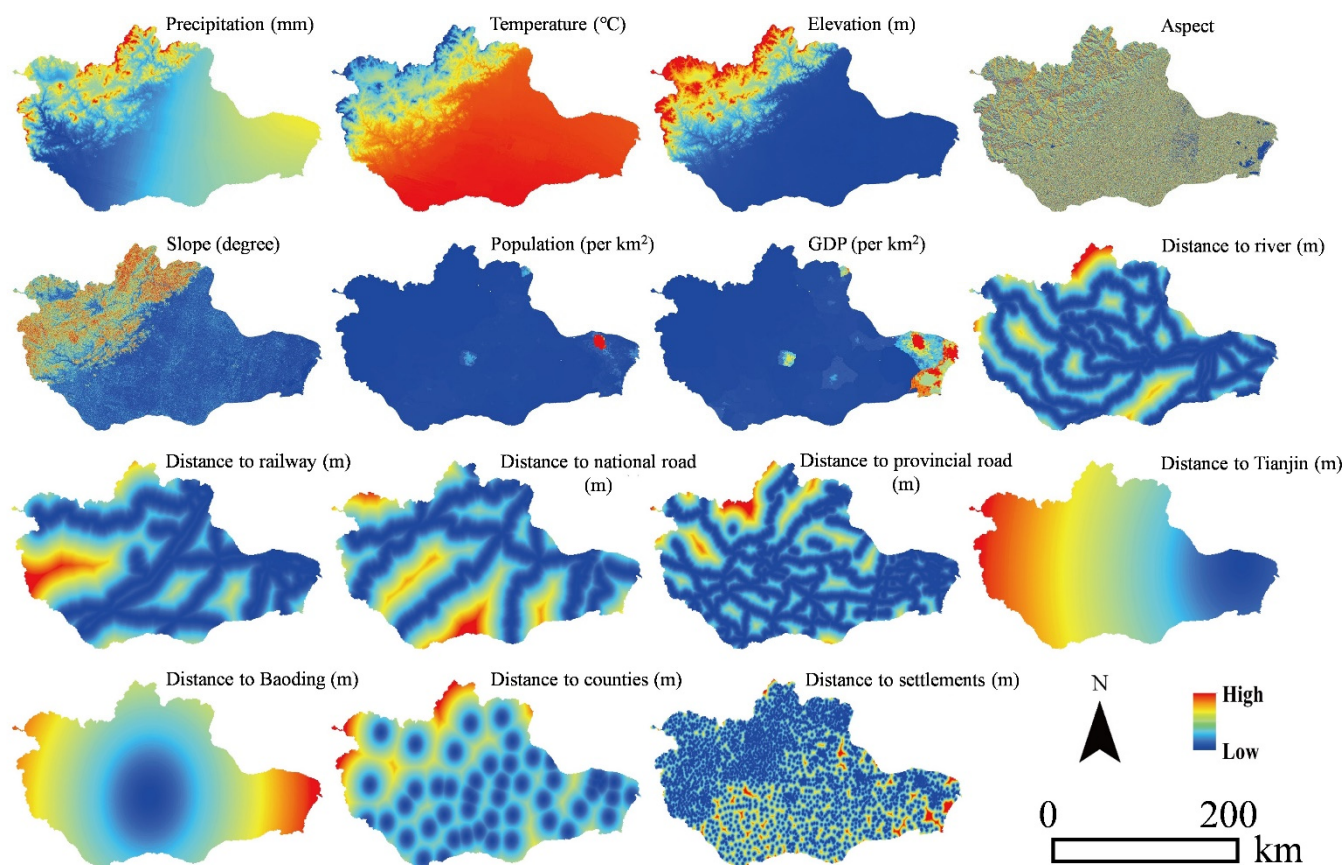


Figure 2. Land use evolution drivers in the Daqing River Basin.

2.3. Methods

In the process of this study, we first classified PLES based on the land use data of the Daqing River Basin, and then made a multi-scenario projection of future land use, followed by an analysis of the changes in PLES and its coupled coordination degree at the overall basin and county unit levels (Figure 3).

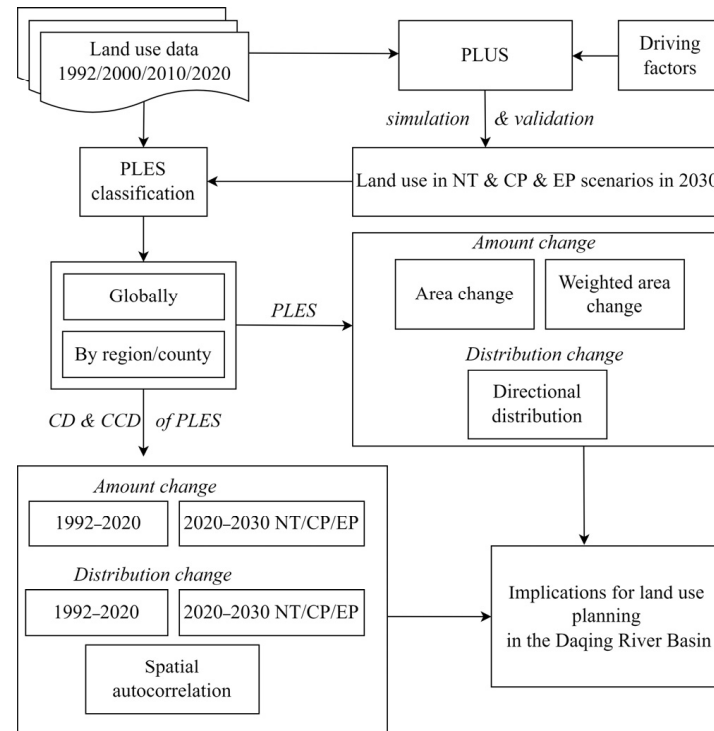


Figure 3. Overall research flow of this study.

2.3.1. Classification of PLES

In the original land use data set of ESA's CCI, the classification of land use was complicated. To facilitate the calculation, we used ArcGIS reclassification function to classify the land use into eight categories: cropland, forest, shrubland, grassland, built-up land, bareland, wetland, and water, with reference to existing related research methods and combined with the actual situation of the Daqing River Basin. Cropland includes paddy fields and dry-farmed land, while forest includes deciduous trees and evergreen trees. Shrubland includes evergreen shrubs and deciduous shrubs. Grassland includes mountain meadows and meadows in the plains. Built-up land includes built-up areas of towns and rural settlements and transportation land. Bareland refers to land that is to be developed and unused and lacks vegetation cover. Wetland includes the wetlands around lakes and river mudflats. Water includes all types of water bodies such as lakes, reservoirs, rivers, and ponds.

In terms of PLES functions of land use, some studies have assigned a single function to each land use type [33,46], while others have taken a more composite view of PLES functions carried by each land use type [47–49]. In order to analyse the transformation of PLES in the Daqing River Basin in more detail, this study adopts a composite perspective and assigns numerical scores to the above eight land use types with reference to previous studies and expert opinions. Each land type has a dominant function, e.g., cropland has a dominant function of providing space for production, and is therefore assigned a value of 5. Cropland also has some ecological functions; however, these are less prominent than those of forest and wetland and are therefore assigned a value of 2 [47,50] (Table 2).

Table 2. PLES functions of various types of land use.

Land Use Type	Production Function	Living Function	Ecological Function	Dominant Function
Cropland	5	0	2	Production
Forest	0	0	5	Ecological
Shrubland	0	0	5	Ecological
Grassland	1	0	5	Ecological
Built-up land	3	5	0	Living
Bareland	0	0	1	Ecological
Wetland	0	0	5	Ecological
Water	0	0	5	Ecological

2.3.2. Coupling Coordination Degree Analysis

According to the definition of CD and CCD calculation formula, the absolute area of PLES needs to be normalized. Considering that there is no negative influence that any PLES type on the CD and CCD, we have normalised PLES data using a non-zero transformed indicator normalisation method, as follows.

$$X_{ij} = \left(\frac{x_{ij} - x_{j \min}}{x_{j \max} - x_{j \min}} \right) \times 0.99 + 0.01 \quad (1)$$

X_{ij} denotes the final value of PLES type j of region i , taking values in the range [0.01, 1]. x_{ij} denotes the original weighted area of PLES type j of region i , and $x_{j \max}$ and $x_{j \min}$ denote the maximum and minimum weighted areas of PLES type j in the year series, respectively.

The coupling degree (CD) refers to the extent of the interaction between multiple components within a system and can therefore be used to express the extent to which PLES functionally contribute to, coerce, and influence each other, as shown by the following formula [51,52].

$$C_d = 3 \times \left[\frac{S_p \times S_l \times S_e}{(S_p + S_l + S_e)^3} \right]^{\frac{1}{3}} \quad (2)$$

CD refers to the coupling degree, and S_p , S_l , and S_e represent the normalised values of production space, living space, and ecological space, respectively, calculated by Equation (1). The values of CD are in the range [0, 1] and are divided into four categories: low coupling period, antagonistic period, break-in period, and coordinated coupling period (Table 3).

Table 3. Grading of CD in the Daqing River Basin.

Value Range	Meaning	Feature
$CD \in (0.8, 1.0]$	Coordinated coupling period	PLESs are highly coupled and PLES functions are in a highly ordered state.
$CD \in (0.5, 0.8]$	Break-in period	Production space, living space, and ecological space are mutually constrained towards orderliness.
$CD \in (0.3, 0.5]$	Antagonistic period	PLES types with a strong position are produced, while other types are weaker.
$CD \in (0.0, 0.3]$	Low coupling period	Production space, living space, and ecological space develop in a disorderly manner with little interaction.

Although the CD can characterise the extent of the interaction between production space, living space, and ecological space, it cannot effectively characterise the degree of coupling coordination among the three; therefore, we used the indicator of the coupling coordination degree (CCD) to analyze the coordination of PLES in the Daqing River Basin [53], and the formula is as follows.

$$CCD = [C_d \times (\alpha S_p \times \beta S_l \times \gamma S_e)]^{\frac{1}{2}} \quad (3)$$

CCD represents the coupling coordination degree of PLES, and α , β , and γ represent the weights of production space, living space, and ecological space. Considering that the Daqing River Basin plays more of a production and living function than other regions in China, for example, the mountainous regions of western China, we assign α , β , and γ to 0.35, 0.35, and 0.3, respectively, taking into account the findings of previous studies [36,54]. C_d , S_p , S_l , and S_e are the same as in Formula (2). The value range of CCD is [0, 1], and, drawing on the basic ideas of fuzzy mathematics, we classify them into five categories, namely severe imbalance, moderate imbalance, basic coordination, moderate coordination, and high coordination [53,54] (Table 4).

Table 4. Grading of CCD in the Daqing River Basin.

Value Range	Meaning	Feature
$CCD \in (0.8, 1.0]$	High coordination	The coexistence of production space, living space, and ecological space is highly coordinated and can meet the needs of different levels of interest.
$CCD \in (0.6, 0.8]$	Moderate coordination	There is a moderate coordination degree among production space, living space, and ecological space.
$CCD \in (0.4, 0.6]$	Basic coordination	The gap between the shares of PLESs has narrowed further and is beginning to produce a positive interaction.
$CCD \in (0.2, 0.4]$	Moderate imbalance	One type of PLES is still dominant, but the share of other types has increased.
$CCD \in (0.0, 0.2]$	Severe imbalance	The dominance of one type of PLES (e.g., living space or production space) squeezes the other spaces.

2.3.3. Land Use Simulation

The analysis of historical changes of land use is the basis of future land use prediction. Logically, the degree and quantity of future land use changes should be related to historical changes. Therefore, it is necessary to analyze the historical land use change first. Here, we used the land use conversion matrix [55] for land use change analysis to gain an insight of the trend of land use transformation in the Daqing River Basin and to establish a basis for subsequent land use projections. The land use transfer matrix can be described as the following formula:

$$P = \begin{bmatrix} p_{11} & \cdots & p_{1n} \\ \vdots & \ddots & \vdots \\ p_{n1} & \cdots & p_{nn} \end{bmatrix} \quad (4)$$

where P represents the land use conversion matrix among different years and the element p_{ij} in the matrix refers to the probability of conversion from land use i to land use j .

Land use prediction can be divided into two parts: one is land use quantity prediction and the other is spatial distribution prediction. We here estimated future land use quan-

tity demand using a Markov model, which has good robustness in a long-time interval forecasting [56]. The Markov model principle can be described as the following formula.

$$D_{t_2} = D_{t_1} \times P^{\frac{t_2-t_1}{a}} \quad (5)$$

where D_{t_2} denotes land use demand at t_2 ; D_{t_1} denotes land use status at t_1 ; and P is the same as described in Equation (4), with a denoting the interval between the starting and ending years for calculating P .

Different future development policies are expressed through different land use conversion probabilities. Observing the land use change history of the Daqing River Basin from 1992 to 2020, it is found that the most prominent features are the increase of built-up land and the reduction of cropland, while, at the same time, there is a consensus to enhance ecological protection. We constructed three development scenarios [11,57,58]: (1) The natural trend development scenario (NT) assumes no major changes in regional development policies, and that future land use will continue the transformation pattern of the previous phase, keeping the probability of previous land use shifts unchanged. (2) Cropland preservation development scenario (CP), which focuses on the protection of cropland and strictly limits the encroachment of cropland by other land use types. On the benchmark of the land use transfer probability matrix for NT, the proportion of cropland transferred to built-up land is reduced by 50%, and the proportion of transfer to forest, shrubland, grassland, and wetland is reduced by 30%, and the lesser part of these transfers is added to the cropland itself. (3) The ecological preservation development scenario (EP) focuses on the conservation of land use types with outstanding ecological functions, such as forest, grassland, and wetland, etc. On the benchmark of the natural trend development land use transfer probability matrix, the proportion of transfer from cropland to built-up land is reduced by 50%, and the decreased portion is added to forest, while the proportion of transfer from forest, shrubland, grassland, and wetland to built-up land is decreased by 30% and the decreased portion is added to their respective land use categories. Previous studies [5,59,60] have generally set the projection time at 10–50 years; however, in this study, we set the projection time at 2030 instead of projecting for later years, considering that an extension of 50 years would produce very large changes with weak practical application and reference value. We used MathWorks MATLAB R2021a programming to implement the above forecasting process.

Due to the combination of advanced machine learning algorithms, the PLUS model can more accurately calculate the probability of land use change than other models [39,40], which has been confirmed in several varied scales studies [41–43]; therefore, we also adopted this model. PLUS adopts the Random Forest Classification (RFC) to calculate the factors driving land use expansion and then uses the CA model to generate land use distribution maps [40]. The formula for the random forest algorithm is as follows.

$$P_{i,k}^d(x) = \frac{\sum_{n=1}^M I(h_n(x) = d)}{M} \quad (6)$$

where $P_{i,k}^d$ refers to the probability of sprawl of site type k at site i ; the value of d is 1 or 0—1 means that the conversion of other sites to site type k has taken place at that site and 0 means no conversion; x is the drivers set; $I(\cdot)$ is the indicator function of the set of decision trees; $h_n(x)$ is the prediction type of the n th decision tree of vector x ; and M is the overall amount of decision trees [40].

The CA model in PLUS combines multi-type random patch seeds and a descending threshold, enabling it to simulate the automatic generation of land patches in a spatio-temporal dynamic manner [61]. The CA model formula is as follows.

$$S_{(t+1)} = f(S_t, N) \quad (7)$$

where S_t and $S_{(t+1)}$ refer to the status of the land use cell at timepoints t and $t + 1$, respectively; N refers to the neighbourhood of the cell, the amount of which can be set by researchers to obtain the optimal training results; and f refers to the land use conversion rule.

We first calculated the spatial distribution of land use change in the Daqing River Basin from 2010 to 2015 by utilising the PLUS model and then combined the driving factors and inputted them into the PLUS Land Expansion Analysis Strategy (LEAS) in the proportion of 70% for the training set and 30% for the validation set to participate in training and validation [40]. The root mean square error (RMSE) and out-of-bag RMSE are used to characterise the effectiveness of the random forest model training. After the model is trained, the simulation results need to be calibrated, and the parameters of the PLUS model need to be determined. The trained model was used to predict the land use distribution in 2020 according to the 2015 land use data. Two indicators, Overall Accuracy and Kappa Coefficient [62], were utilised to calculate the accuracy of the predicted land use in 2020 and to determine whether the model was ideal for predicting the future land use distribution in the Daqing River Basin.

2.3.4. Spatial Distribution Characteristics Analysis of PLES

Given that the analysis period in this study spans nearly 40 years, the trend of the PLES spatial distribution is a feature that needs to be made explicit. The standard deviation ellipse [63] is robust in presenting the directional characteristics of the analysed elements, we used this algorithm to analyse the central, discrete, and directional trends of the PLES spatial distribution. The long axis of the ellipse refers to the direction of the expansion of the PLES distribution, while the short axis represents the extent of the distribution; moreover, the larger the flatness of the ellipse, the more directional the PLES distribution is. This analysis was carried out using the Directional Distribution tool in ArcGIS 10.8.1.

We used global Moran's I [64] to examine the spatial trend of CCD both from 1992 to 2020 and in 2030. Then we analysed the differences among them. global Moran's I can be described by the following formula.

$$I = \frac{n \sum_{i=1}^n \sum_{j=1}^n \omega_{ij} (P_i - P_{mean}) \times (P_j - P_{mean})}{\left(\sum_{i=1}^n \sum_{j=1}^n \omega_{ij} \right) \times \sum_{i=1}^n (P_i - P_{mean})^2} \quad (8)$$

I represents the global autocorrelation index and takes values in the range of $[-1, 1]$, $I > 0$ means that elements with close values have clustered in space, $I < 0$ means that elements with considerable differences in values cluster in space, while $I = 0$ indicates that there is no spatial correlation in the distribution of elements. P_i and P_j denote the values of sample i and sample j , n denotes the number of samples, P_{mean} denotes the sample mean, and ω denotes the spatial weight matrix.

In addition, we used local Moran's I [65] to analyse the spatial variability of the CCD distribution with the formula shown below.

$$\text{Local Moran}'I = \frac{n(P_i - P_{mean}) \sum_{j=1}^m \omega_{ij} (P_j - P_{mean})}{\sum_{i=1}^n (P_i - P_{mean})^2} \quad (9)$$

where m refers to the number of samples adjacent to sample i . The meaning of the remaining indicators is the same as in Equation (8).

3. Results

3.1. Outcomes of Land Use Simulation Experiment

3.1.1. Land Use Modeling Accuracy

The results of the random forest model training indicated that the root mean square error (RMSE) of the prediction results for all eight land use types was less than 0.1. The values of out-of-bag RMSE for cropland, forest, grassland, and built-up land ranged from

0.1 to 0.18, and the values of out-of-bag RMSE for shrubland, bareland, wetland, and water were all less than 0.1 (Table 5). The values of the above two types of parameters indicate that the random forest model proposed in our study has high training accuracy, the model training results are highly ideal, and the land use expansion suitability obtained has high confidence. Comparing the actual land use distribution in 2020 with the simulated land use distribution in 2020 (Figure 4), the Overall Accuracy and Kappa Coefficient were 0.96 and 0.94, respectively, indicating that the land use simulation model trained in this study is highly accurate and suitable for future land use prediction in the Daqing River Basin.

Table 5. Training accuracy of the random forest model in PLUS.

	Cropland	Forest	Shrubland	Grassland	Built-Up Land	Bareland	Wetland	Water
RMSE	0.064056	0.054236	0.032019	0.039796	0.040792	0.034185	0.028695	0.017367
OOB RMSE	0.171688	0.157187	0.079088	0.108348	0.121637	0.085938	0.085787	0.056324

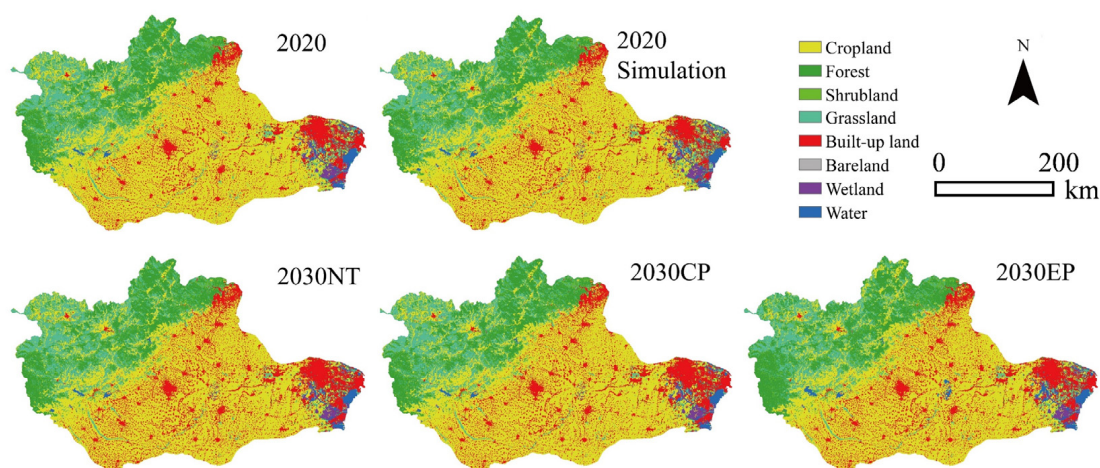


Figure 4. Land use distributions of 2020 actual, 2020 simulated, and different development scenarios under 2030.

3.1.2. Land Use in 2030 under Three Different Development Scenarios

Compared to 2020, the 2030 NT, CP, and EP scenarios show a rise of forest, built-up land, and bareland, and a decrease of cropland, shrubland, grassland, wetland, and water. The built-up land increases the most, by 1350.45 km², 899.99 km², and 851.44 km² under the three scenarios, an increase of 23.57%, 15.71%, and 14.86%, respectively. The area of cropland decreased the most, by 983.33 km², 474.31 km², and 983.33 km² under the three scenarios, with a decrease of 3.93%, 1.90%, and 3.93% respectively. The area of forest increased the most under EP, by 535.20 km². Shrubland, bareland, wetland, and water changed by smaller and similar amounts under the three scenarios (Figure 4, Table 6).

Table 6. Quantity changes in land use under different development scenarios of 2030.

	Cropland /km ²	Forest /km ²	Shrubland /km ²	Grassland /km ²	Built-Up Land/km ²	Bareland /km ²	Wetland /km ²	Water /km ²
2030 NT	24,032.80	5976.34	1126.83	6220.04	7079.99	11.85	364.68	449.70
2030 CP	24,541.82	5971.33	1124.58	6169.99	6629.53	11.85	364.68	448.45
2030 EP	24,032.80	6450.46	1127.88	6220.04	6580.99	11.85	385.65	452.55
2030NT-2020	−983.33	61.08	−47.27	−300.16	1350.45	0.28	−56.18	−24.90
2030CP-2020	−474.31	56.08	−49.52	−350.21	899.99	0.28	−56.18	−26.15
2030EP-2020	−983.33	535.20	−46.21	−300.16	851.44	0.282	−35.20	−22.05

3.2. Changes of Production–Living–Ecological Space

3.2.1. Changes in the Amount of PLES from 1992 to 2020

Dividing PLES categories of each type of land according to the dominant function, the results show that, between 1992 and 2020, the production space and ecological space in the Daqing River Basin show a monotonic decreasing trend, while the living space shows a monotonic increasing trend (Figure 5). During this time period, the area of production space is always the largest, and the area of living space is always the smallest; however, the gap between the three categories of space is gradually decreasing. Living space increased from 1472.72 km² to 5729.54 km², an increase of 289.04%, and the rate of increase accelerated significantly after the year 2000. Production space decreased from 28,075.45 km² to 25,016.13 km², a decrease of 10.90%, and the rate of decrease accelerated after 2000. The absolute amount of change in ecological space is relatively small, at 1197.48 km², with a decrease of 7.62% and a more constant rate of decrease.

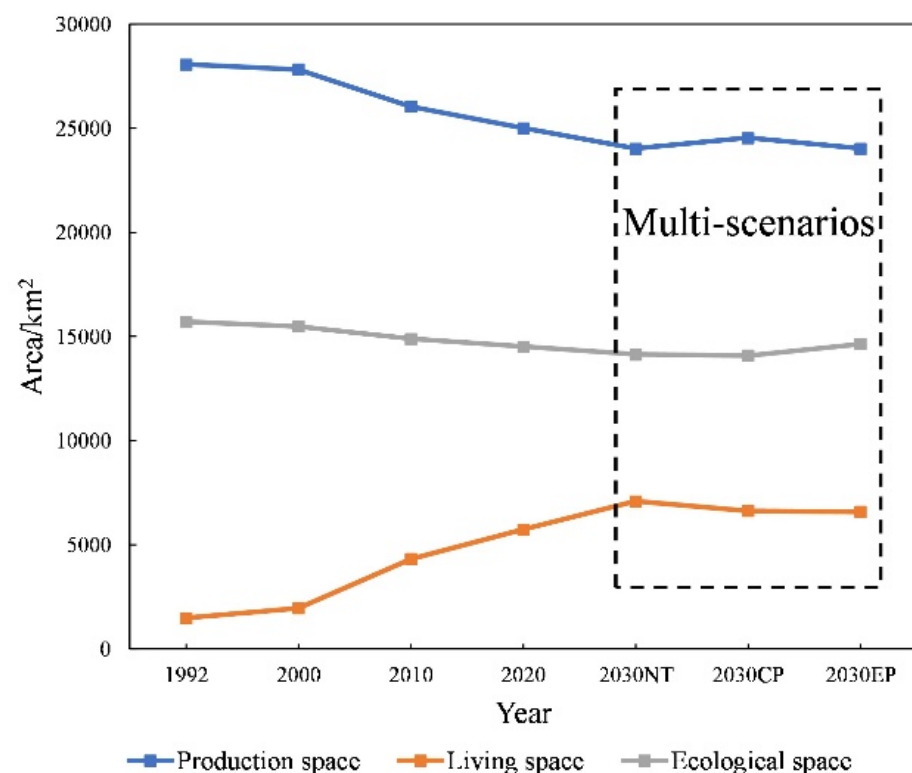


Figure 5. The number of PLES in the Daqing River Basin in 1992, 2000, 2010, 2020, and three different development scenarios of 2030.

The area of PLES in the Daqing River Basin from 1992 to 2020 was computed by weighting the composite function score (Table 2) for each type of land use (Figure 6). The results show that the trends of production space, living space, and ecological space are the same as when they were divided according to the dominant functions; however, the decrease in production space is significantly smaller, with a decrease of only 2.28%. The increase in living space remains at 289.04%, and the decrease in ecological space is 9.01%, which is a slight increase compared to the decrease according to the dominant function.

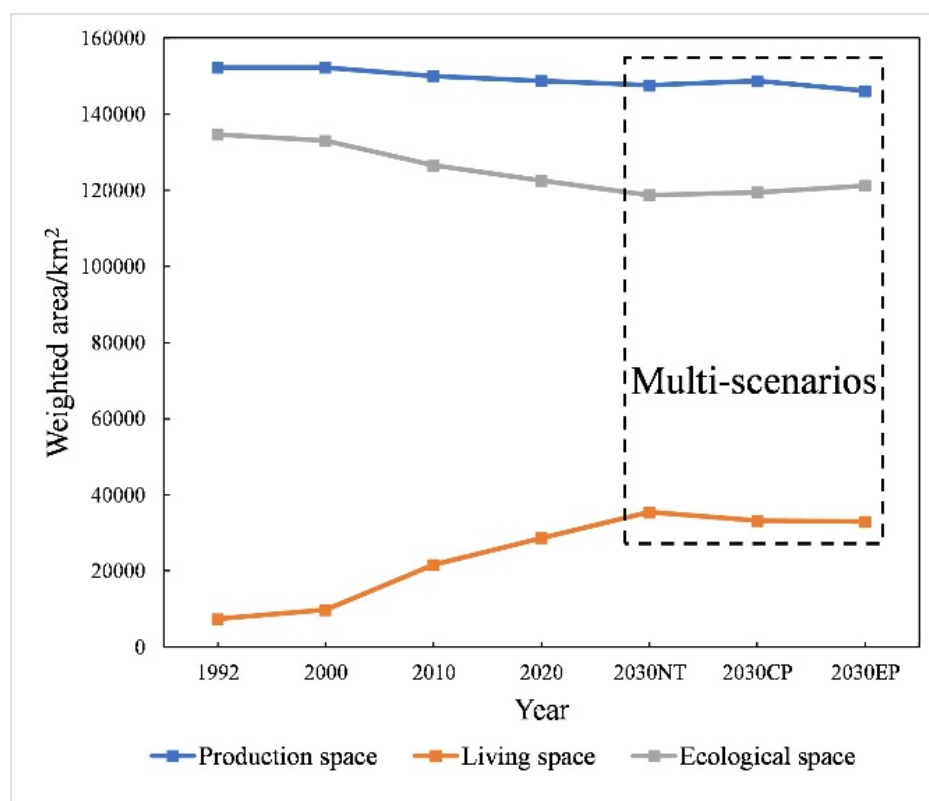


Figure 6. The weighted number of PLES in the Daqing River Basin in 1992, 2000, 2010, 2020, and three different development scenarios of 2030.

3.2.2. Changes in the Amount of PLES under Different Development Scenarios in 2030

When PLES are divided according to the dominant functions, the changes in the area of production–living–ecological areas in 2030 are complex for the three development scenarios. Compared to 2020, under NT, the area of production space and ecological space continues to shrink at a greater rate, while the area of living space continues to grow at a higher rate. Under CP, the area of production space decreases at a lower rate, ecological space decreases at a higher rate, and the growth rate of living space slows down significantly. Under EP, the area of production space decreases at the same rate as NT, while the area of ecological space increases and the growth rate of living space decreases further. We also calculated the area of PLES in the Daqing River Basin for 2030's multi-scenarios by weighting the composite function score for each land use types (Figure 6). The results show that, compared to 2020, the area of production space only decreases more under EP, while the area of ecological space decreases under all three scenarios.

3.2.3. Spatial Distribution Characteristics of PLES

The production space, living space, and ecological space of the Daqing River Basin each have distinctive distribution characteristics (Figure 7). The production space extends along the northwest–southeast direction and has a large distribution, covering all the major zones of the basin. As the flatness of the standard deviation ellipse is small, the directionality of the production space distribution is not prominent, indicating that the production space is distributed relatively evenly within the basin, and the production activities in the basin are widely distributed. After 1992, the spatial distribution of production space shifts towards the southeast side. Considering that cropland in the southeastern part of the basin is actually shrinking, this shift is due to the high-intensity sprawl of built-up land in the southeastern region. Living space is distributed along the northeast–southwest direction, with dense distribution in the middle and east of the basin and sparse distribution in the West. After 1992, the living space also shifted towards the southeast, indicating that

built-up land in the southeast of the basin expanded more than the northwest after 1992. Ecological space is distributed along the northwest–southeast direction with relatively larger elliptical flatness. From 1992 to 2020, an eastward shift in ecological space occurs, indicating that the eastern part of the ecological space is more built up than the western part during this period. The distribution of ecological space will hardly change from 2020 to 2030 EP. From 2020 to 2030 NT/CP, ecological space will shift further eastwards, implying that the ecological space in the western mountainous areas will be more affected under the above two development scenarios.

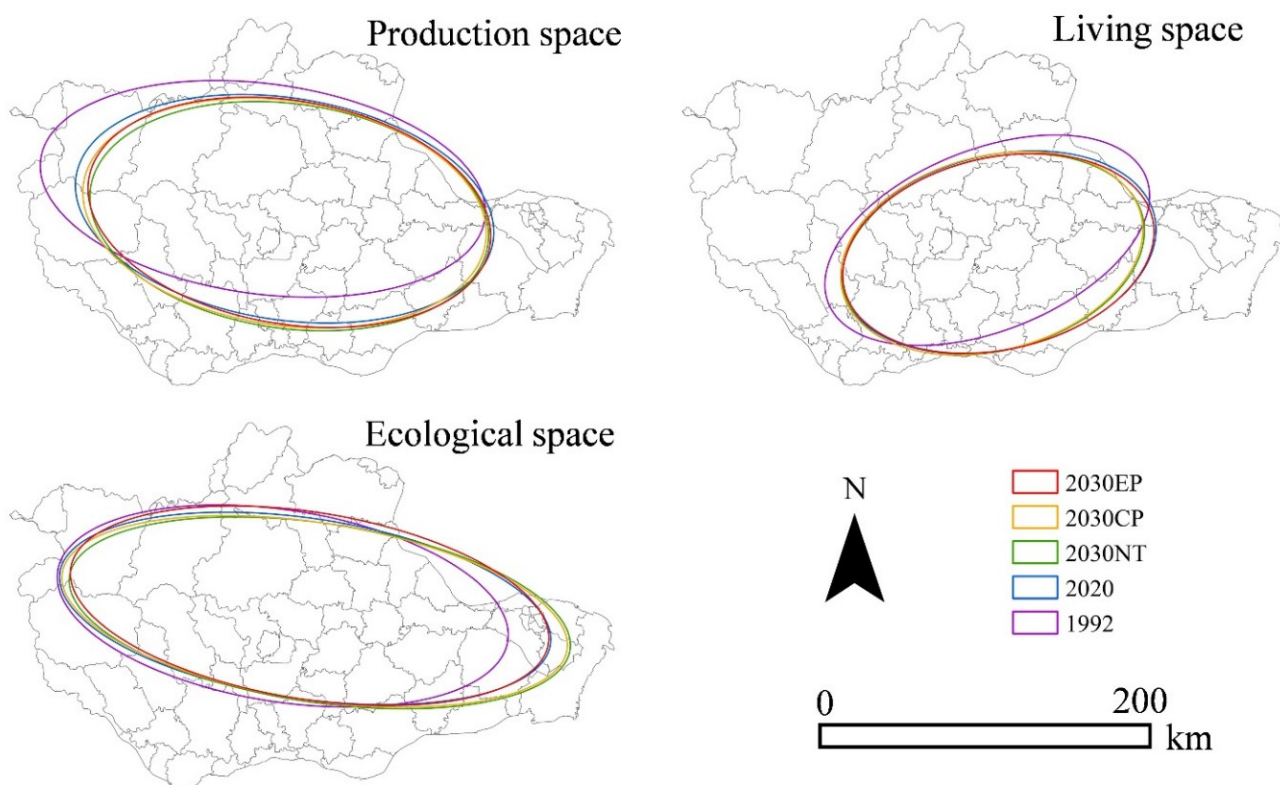


Figure 7. The direction and extent of the distribution of PLES.

3.3. Coupling Degree and Coupling Coordination Degree of PLES

3.3.1. CD and CCD of PLES from 1992 to 2020

Overall, both the CD and CCD of the Daqing River Basin experienced an increase and then a decrease between 1992 and 2020 (Figure 8). The CD value in 1992 was 0.32, indicating that PLES in the Daqing River Basin were just emerging from a low coupling period into an antagonistic period, with the production and ecological spaces in a strong position; however, the interaction with the living spaces had already begun. In 2000, the CD value was 0.66, and the three living spaces were in a break-in period. In 2010, the CD value was 0.99, indicating that the three living spaces were in a highly coupled state, with production, living, and ecological functions functioning in an orderly manner. In 2020, the CD value drops to 0.90, indicating that, as the production and ecological spaces shrink and the living space continues to grow, the highly coupled state between PLES is broken, and the healthy interaction between them is compromised. In 1992, the CCD value was 0.46, and the relationship between PLES in the Daqing River Basin was basically coordinated, with a weak positive interaction. In 2000 and 2010, the CCD values were 0.66 and 0.74, respectively, and PLES were in a moderate status of coordination, indicating that the growth of living space and the reduction of ecological and production space did not cause extreme negative consequences, but rather promoted the interaction between PLES. In 2020, the CCD value drops to 0.67, indicating that, as the living space expands and the production and ecological space shrinks, the coordination between PLES is broken and

the production and ecological functions gradually begin to run the risk of not being able to effectively meet the needs of society. Compared to the 2010 CD value of 0.99, the CCD of the Daqing River Basin has never been greater than 0.8, which means that PLES have never been in a highly coordinated state, indicating that the share of each of the three living spaces in the past development history was not rational.

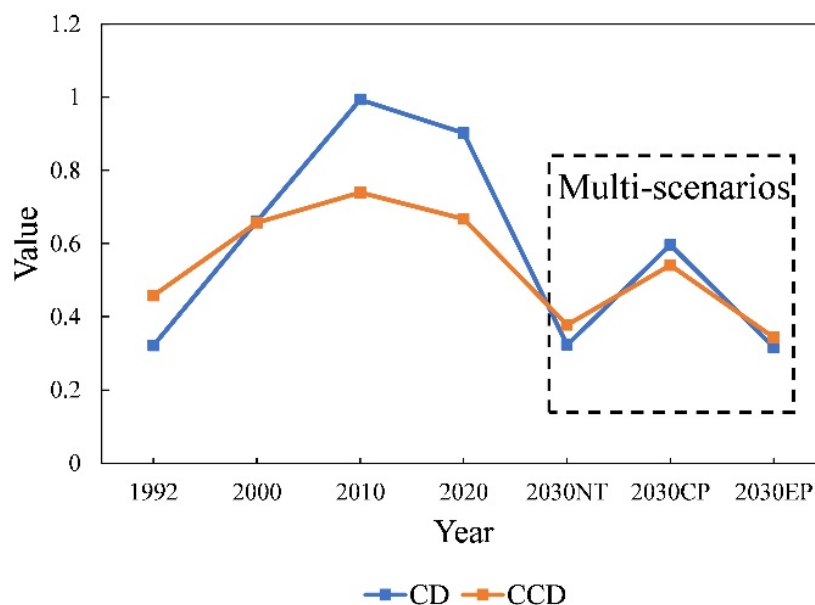


Figure 8. Changes in CD and CCD of the Daqing River Basin.

Consistent with the overall CD and CCD changes in the Daqing River Basin during 1992–2020, the CD and CCD of the 66 county level units in the Daqing River Basin also basically went through a process of increasing and then decreasing, taking 2010 as the boundary (Figures 9 and 10). In 1992, the values of CD and CCD in all 66 county level units were relatively uniform and stable at about 0.32 and 0.45, respectively, indicating that most counties were in the antagonistic period and basically coordinated in PLES; however, there were some counties with extremely low or high values. The large differences in CD and CCD among counties in 2000, 2010, and 2020 indicate that the development evolution of PLES in different counties after 1992 varies greatly due to the influence of policy orientation and local natural endowments, etc. The CD and CCD of each county in 2010 were at their best from 1992 to 2020, basically greater than 0.9 and 0.7, respectively. The bell-shaped distributions of CD and CCD indicate that, under the rapid economic development and previous policy guidance, the PLES of the Daqing River Basin had reached the peak of coordination around 2010, and then the economic construction continued to develop, but that the lack of PLES optimization measures had brought a negative impact.

3.3.2. CD and CCD of PLES under Different Development Scenarios in 2030

Overall, the CD and CCD in the River Basin decline significantly in 2030 compared to 2020 under the three different development scenarios. Under the NT and EP scenarios, the CD and CCD do not differ significantly, both falling back to 1992 levels, while, under the CP scenario, the CD and CCD are significantly higher than under the NT and EP scenarios, and are similar to the levels in 2000 (Figure 8).



Figure 9. Changes in CD and CCD at the county level.

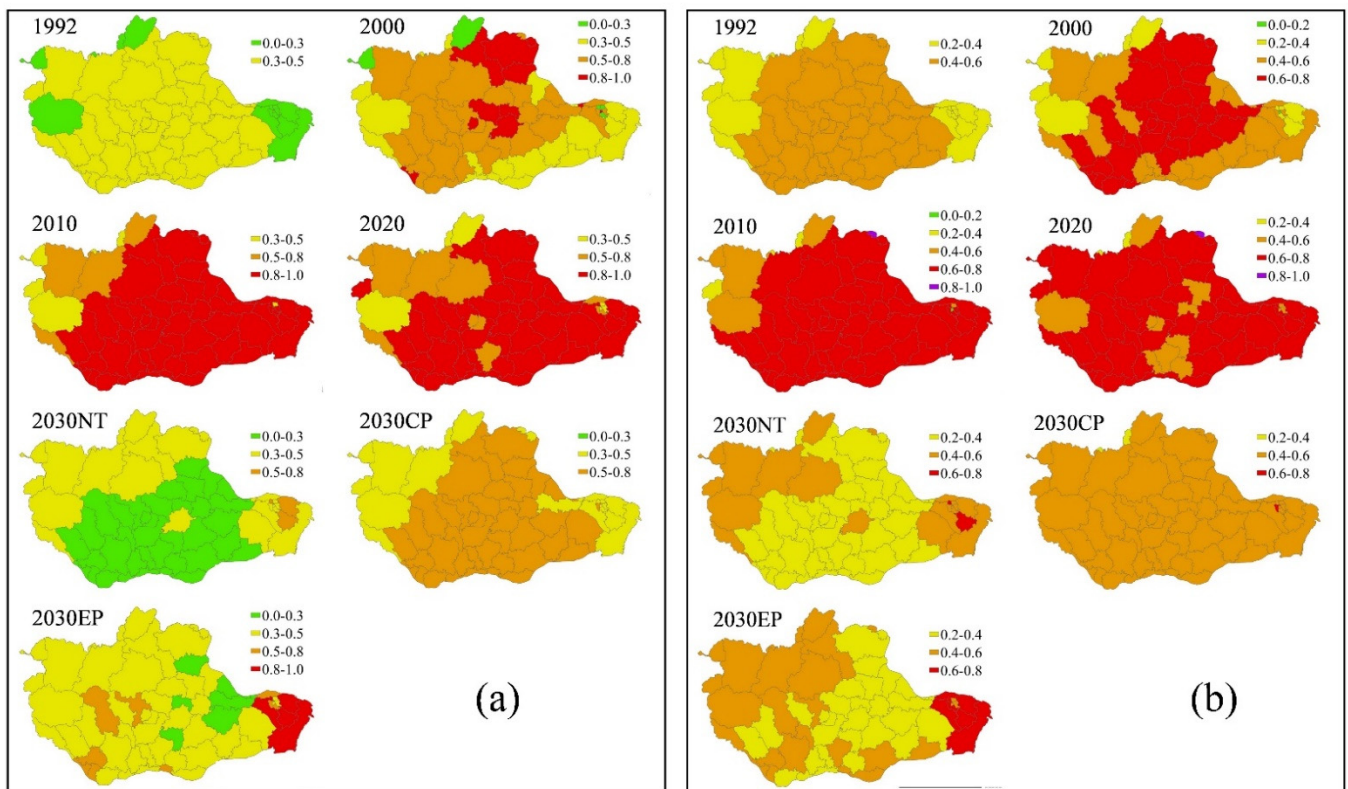


Figure 10. Spatial distribution of CD (a) and CCD (b) at the county level.

By county, in 2030, the vast majority of counties have CD and CCD values ranked from high to low as CP, EP, and NT (Figure 9). Under the 2030 NT scenario, the central part of the Daqing River Basin is in the low coupling period, while the eastern and western parts are in the antagonistic period, with the central city of Tianjin in the break-in period. The 2030 CP scenario is the opposite of the NT scenario, with the central part in the break-in period and the eastern and western parts in the antagonistic period. The distribution of CDs in the 2030 EP scenario is less regular, with antagonistic periods dominating in the central and western regions of the city, interspersed with a few low coupling periods and break-in periods, while the eastern part of the city is in the coordinated coupling periods. In terms of CCD, under the 2030 NT scenario, the central part of the river basin is in moderate imbalance, while the eastern and western parts are in basic coordination, with a small part of the eastern area in moderate coordination. Under the CP scenario, almost all of the Daqing River Basin is in basic coordination, with only Nankai District in Tianjin and Weixian County in Hebei Province in moderate coordination and moderate imbalance, respectively. In the EP scenario, the eastern part is in moderate coordination, the central part is in moderate imbalance and the western part is in basic coordination (Figure 10).

3.3.3. Spatial Autocorrelation Features for CD and CCD of PLES

(1) Global Spatial Autocorrelation Features

The Daqing River basin was divided according to county-level units and the spatial autocorrelation characteristics of CD and CCD were calculated. The results show that, between 1992 and 2020, the spatially positive correlation characteristics were always present in the CD values of the Daqing River Basin. The highest CD value in 2010 corresponds to the year with the weakest spatial positive correlation characteristics, while, in years with the lower CD values, the positive correlation characteristics are stronger. Under the 2030 NT, CP, and EP scenarios, CD still has positive correlation characteristics, and the positive correlation characteristics under NT and CP strengthen compared to 2020, while EP weakens relative to 2020. The spatial correlation of the CCD in the Daqing River Basin varies widely between 1992 and 2020, with 1992, 2000, and 2020 all showing positive spatial correlation, while 2010 has a negative spatial correlation feature. In the 2030 NT and EP scenarios, the CCD is spatially positively correlated, while, in the CP scenario, it is spatially negatively correlated (Table 7).

Table 7. Global spatial autocorrelation results for CD and CCD of the Daqing River Basin at county level.

Type	Year	Moran's I	Z-Score	p-Value
CD	1992	1.38	18.61	<0.01
	2000	0.17	2.47	<0.01
	2010	0.13	1.95	<0.05
	2020	0.50	7.03	<0.01
	2030NT	0.77	10.60	<0.01
	2030CP	0.70	9.43	<0.01
	2030EP	0.41	5.66	<0.01
CCD	1992	1.48	19.94	<0.01
	2000	1.04	14.04	<0.01
	2010	−0.01	2.12	<0.05
	2020	0.02	2.50	<0.05
	2030NT	1.03	13.84	<0.01
	2030CP	−0.05	1.96	<0.05
	2030EP	0.96	13.12	<0.01

We further examined the relationship between the overall CD or CCD of the Daqing River Basin and the spatial autocorrelation features of the CD or CCD at county level. The results showed that, as the overall CD or CCD of the watershed increased, the spatial positive correlation characteristics between the CD or CCD of the county decreased accordingly, with significant p values of 0.003837792 and 0.000359247, respectively, both meeting the 99% confidence level for the p value requirements (Figure 11).

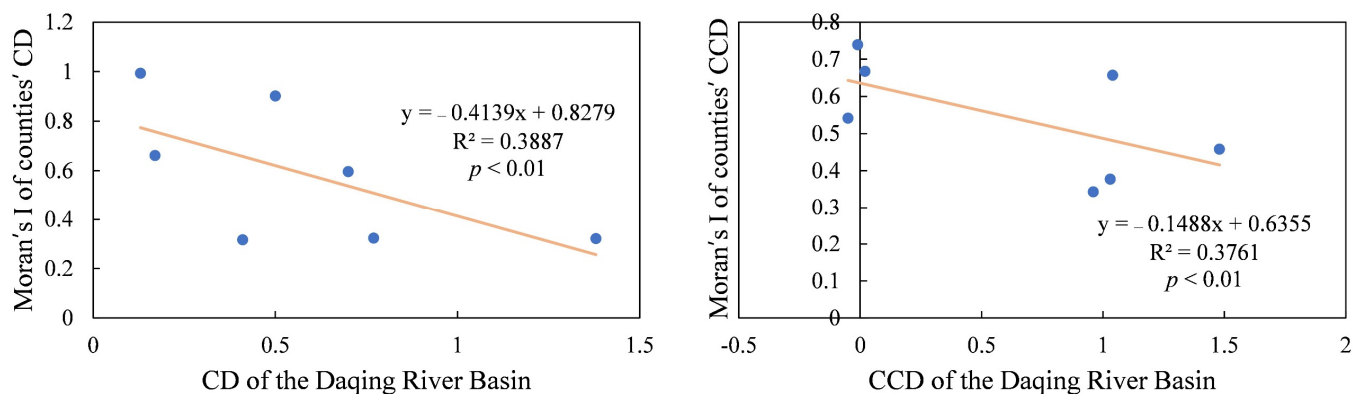


Figure 11. Left: relationship between the global Moran's I of counties' CD and CD of the Daqing River Basin. Right: relationship between the global Moran's I of counties' CCD and CCD of the Daqing River Basin.

(2) Local spatial autocorrelation features

The global spatial autocorrelation analysis reveals the overall CD and CCD distribution characteristics of the Daqing River Basin, but it is difficult to portray the regional differences in CD and CCD distribution characteristics in more detail, therefore we continued to use counties as units to carry out local spatial autocorrelation analysis of CD and CCD. During the period 1992–2020, the high-value CD in the central part of the Daqing River Basin has been characterised by a significant positive spatial correlation; however, the specific location has changed somewhat, reflecting a shift from the northeast to the southwest side. Low-value CD in 1992–2020 are spatially positively correlated in the east and west. Meanwhile, low–high and high–low clusters of CD in 1992–2020 are mainly distributed in the east and west. In the 2030 CP scenario, the central part of the Daqing River Basin is still a spatially positively correlated region for high-value CD, while the eastern and western parts are still spatially positively correlated for low-value CD. In the 2030 NT and EP scenarios, the spatially positive correlated high-value CD area shifts to the eastern part of the basin, while the spatially positive correlated low-value CD area shifts to the central part of the basin. The high-value CCD in the central part of the Daqing River Basin is characterised by positive spatial correlation in 1992 and 2020, shifting to the east in 2010, while there is no positive spatial correlation area for the high value CCD in 2020. Between 1992 and 2020, the low-value CCD spatially positively correlated areas are mostly distributed in the western and eastern parts of the basin, with no distribution in the central part. In the 2030 CP scenario, the low-value CCD spatially positively correlated areas are mostly located in the western part of the basin. In the 2030 NT and EP scenarios, compared to 2020, the spatially positive correlated high-value CCD areas shift to the east and west, while the spatially positive correlated low-value CCD areas shift to the central part of the basin (Figure 12).

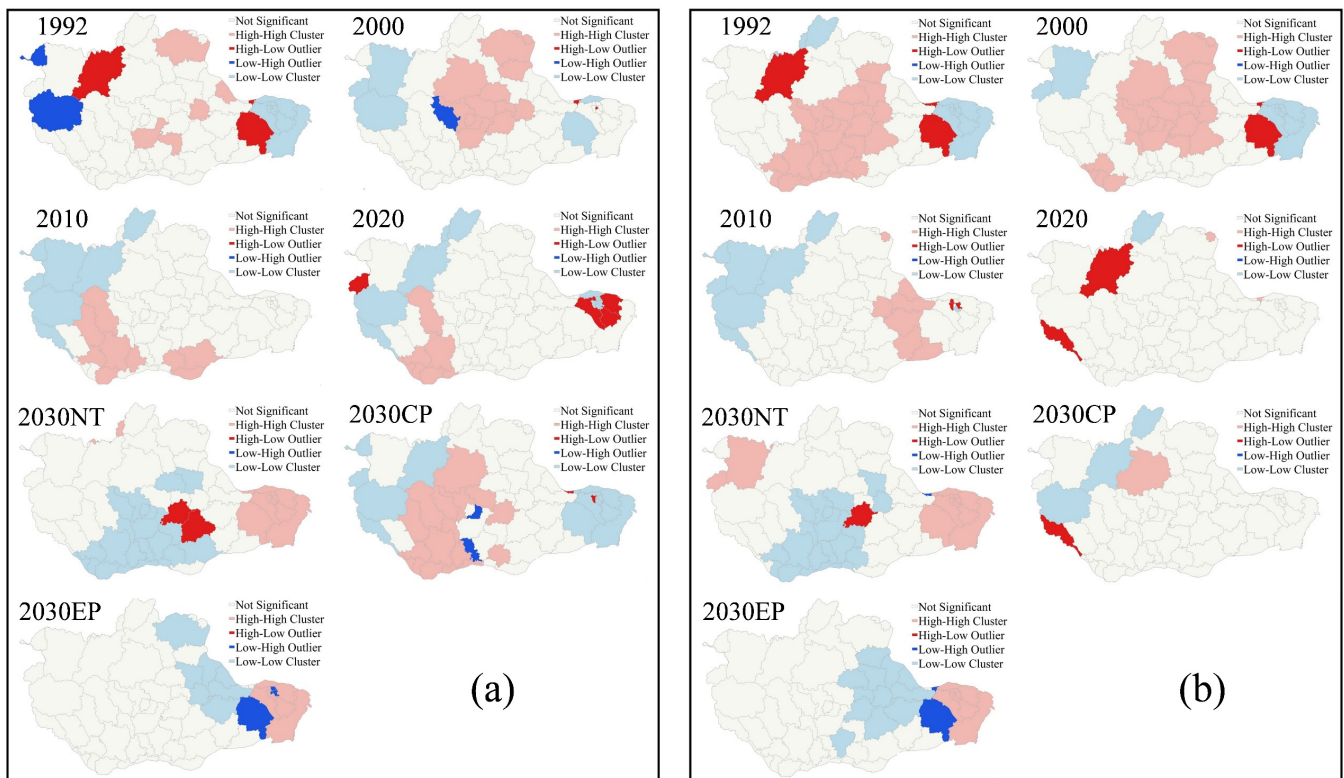


Figure 12. Local Moran's I of CD (a) and CCD (b) at county level in 1992, 2000, 2010, 2020, and three development scenarios of 2030.

3.3.4. Features of Changes for CD and CCD

(1) Changes from 1992 to 2020

From 1992 to 2020, both CD and CCD showed an increasing trend in all counties of the Daqing River Basin. In terms of CD, the eastern region has the largest increase in CD, mostly between 0.6 and 0.8; however, the increase in the central urban area of Tianjin (including Hebei, Hedong, Hexi, Heping, and Nankai districts) is smaller; the increase in the counties in the central region is mostly between 0.4 and 0.6; and the increase in the counties in the west varies greatly; for example, the increase in Fuping and Weixian counties is in the range of 0.0–0.2. In the western counties, the increase was more varied, e.g., 0.0–0.2 in Fuping and Weixian and 0.6–0.8 in Xingtang. In terms of CCD, the eastern counties show a considerable increase in values between 0.4 and 0.6. The central counties show a small increase in values between 0.0 and 0.2. The western counties show varied changes in values, the northwestern counties show an increase between 0.2 and 0.4, and the southwestern counties show an increase between 0.0 and 0.2 (Figure 13).

(2) Changes from 2020 to 2030

Relative to 2020, the CD declines in the vast majority of the Daqing River Basin under the 2030 NT, with the greatest declines occurring in the south-central part of the basin, mostly between 0.6 and 1.0, though with increases in Tang and Weixian counties. The spatial distribution of changes in CCD is generally consistent with CD, with the largest decreases in the south-central part of the basin, with values ranging from 0.4 to 0.6. Under the CP scenario, CD values decreased in all counties of the Daqing River Basin except for Weixian, with the largest decrease in the east, ranging from 0.4 to 0.8, and a smaller decrease in the central counties, ranging from 0.0 to 0.4. Under the CP scenario, all counties, except Xingtang, experienced a decrease in CCD values, with larger decreases in the eastern counties and smaller decreases in the central and western counties. Under the EP scenario, the CD in the central counties of the Daqing River Basin decreased significantly. In terms

of CCD, the decline was also relatively large in the central counties, ranging from 0.2–0.4, while the decline in the eastern and western counties ranged from 0.0–0.2 (Figure 13).

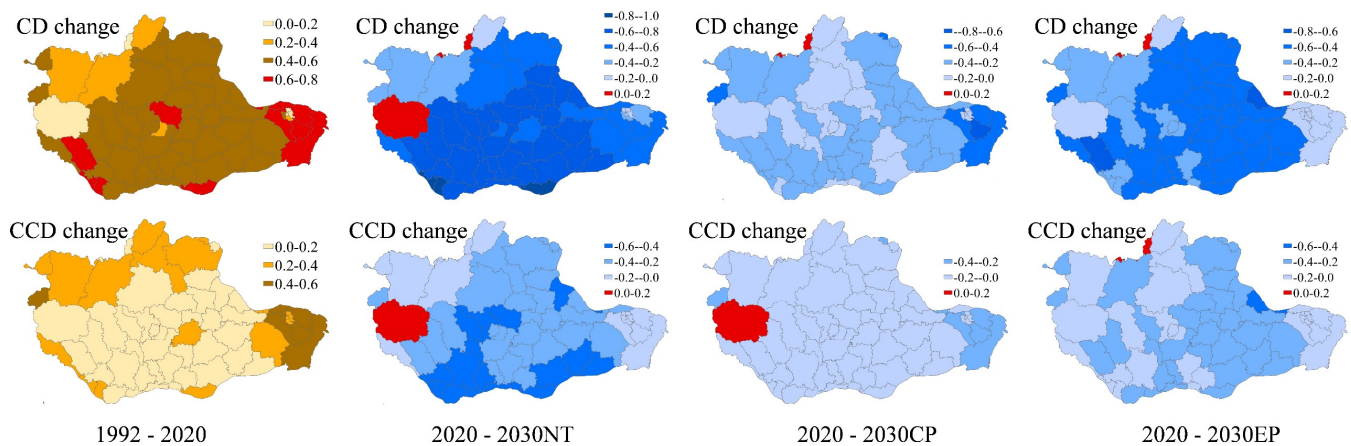


Figure 13. Changes in the spatial distribution of CD and CCD in county level.

4. Discussion

According to our study, from 1992 to 2020, the CD and CCD of PLES of the Daqing River Basin has undergone a “bell-shaped” change. According to the CCD, 2010 was the most coordinated period for the relationships among PLES in the river basin, and, after this period, the CCD of PLES gradually declined to the level of 2000, and will continue to decline if the development trend remains unchanged. This phenomenon also exists in some other study areas, such as the Fen River Basin in China [37]. The change in the CCD of PLES reflects the change from the functional surplus to functional saturation to functional deficiency of the land use in the Daqing River Basin as the social and economic development continues [66]. Especially after 2010, the scale of the land use is still able to meet the requirements of economic development, and this is reflected in the continuous expansion of the built-up land; however, it is no longer possible to support the coordination between production, living, and ecological functions. In terms of social development patterns, the previous development policies of the administrative space in which the river basin is located have had a saturating effect on land use since around 2010 [67,68]. For the sake of coordinating PLES, it is essential to adjust the previous unsustainable development pattern characterised by incremental expansion. The Daqing River Basin needs to focus on a stock development strategy to control the amount of built-up land and to improve the quality and sustainability of social development.

At the county scale, the course of CCD change is consistent with the basin as a whole, which also undergoes an upward and then a downward process. Nevertheless, the magnitude of change varies significantly between counties, and counties with similar magnitude of change are spatially clustered, e.g., counties with the greatest change in CCD values are concentrated in the eastern part of the Daqing River Basin, while counties with relatively small change in CCD values are concentrated in the central part of the basin. Since the eastern, central, and western parts of the river basin have very different economic development patterns and levels, the spatial clustering of counties with similar changes in CCD values reflects that the spatial changes in PLES are not random, but instead are closely related to the regional development status.

We observed in our study that, as the overall CD or CCD in the Daqing River Basin rises, the positive spatial correlation of CD or CCD at the county level gradually decreases. In terms of spatial patterns, from 1992 to 2020 and then to 2030, the Daqing River Basin experiences an uneven state, a relatively balanced state, and an uneven state of CD and CCD distribution (Figure 14). This reflects the spatial effect of spatial variation in PLES of the Daqing River Basin, and the positive correlation between the equilibrium of PLES of the basin as a whole and the equilibrium of PLES’s CCD of the county groups. The imbalance

in the overall spatial distribution of PLES in the basin can be reflected in the relationship between county groups, while the imbalance in the spatial distribution of county groups' CD or CCD also shapes the spatial imbalance of PLES in the basin as a whole.

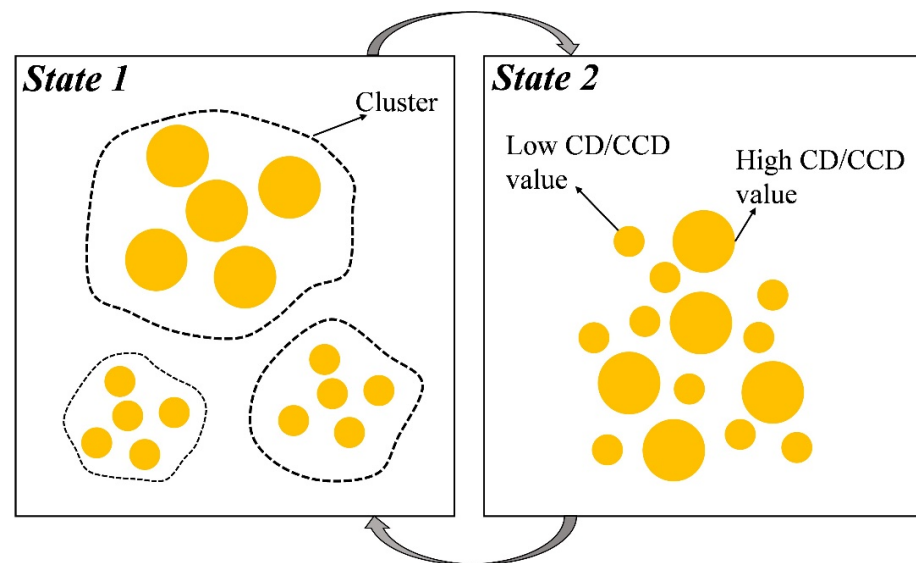


Figure 14. The state conversion of CD and CCD in the Daqing River Basin.

For the optimisation or maintenance of the CCD of PLES, a policy such as returning cropland to forest is not necessarily the best policy, as the policy should be region-specific and problem-specific. Although ecological conservation policies can help to promote the ecosystem service capacity of the Daqing River Basin, and, in many other areas, is a development strategy to maintain the CCD of PLES [69], taking into account the needs of socio-economic development and the CCD of PLES, the best development strategy for the Daqing River Basin may be to enhance the preservation of cropland. Considering that the protection of cropland will inevitably reduce the transfer of cropland to built-up land, it is crucial to optimise the current built-up land in the future.

Whether it is the changes in PLES from 1992 to 2020 or in the three different development scenarios in 2030, it is easy to observe that the eastern, central, and western parts of the Daqing River Basin are three sub-regions with distinctive characteristics. PLES changes in these three sub-regions have had different impacts on human well-being within them over the course of their history. The rapid rise in CCD in the east has corresponded with rapid regional economic development, objectively raising the income levels of local people [70]. The CCD in the west has been at a relatively low level, and there is still latent capacity for further advancement. Under the 2030 NT and EP, the CCD of PLES in the central part of the Daqing River Basin is significantly more affected than those in the eastern and western parts of the basin. Under the 2030 CP, the impacts on the eastern, central, and western CCDs are more balanced. Therefore, in addition to considering the basin as a whole, it is also imperative to devote to the actual situation of the sub-regions and use PLES as a resource with which to promote the socio-economic level of the region. While our study has projected the future spatial changes of PLES for the Daqing River Basin as a whole, a multi-scenario projection of the spatial changes of PLES for each of the sub-regions of the Daqing River Basin will help to identify the development strategies that are most conducive to improving the CCD of the sub-regions. Therefore, the role of scale effects in prediction needs to be addressed in subsequent studies [33,71].

We were devoted to exploring the spatial evolution of PLES in the Daqing River Basin over a long time series; however, due to the limitation of land use data sources, we used data with a resolution of 300 m; thus, some small built-up land (e.g., small villages), wetlands, and water (e.g., small ponds around villages) may be overlooked, which leads to some uncertainty in the analysis results. In the future, with more abundant data sources,

data with higher spatial resolution (e.g., 30 m) can be utilised to study the spatial variability of PLES in the area to further enhance the credibility of the results. In addition, although we have made detailed reference to the data selection methods of existing studies, and combined with the data availability of the Daqing River Basin, we have finally identified the drivers of land use dynamics. However, as the drivers of land use change are extremely complex, the selection of drivers in any one study cannot be perfect, and our study is no exception.

5. Conclusions

The main aim of this study is to explore the historical changes and future development direction of PLES in basins with high economic development so as to provide new insights for the high-quality sustainable development of basins. In order to achieve these objectives, we classified PLES in the Daqing River Basin according to land use data, calculated the changes in the number, CD, and CCD of PLES from 1992 to 2020, and analysed the spatial distribution characteristics of PLES. We then integrated the CA model and PLUS model to make multi-case scenario projections of land use in the Daqing River Basin in 2030, on the basis of which we analysed the evolution directions of PLES in the basin. Our results show that the living space in the Daqing River Basin continues to expand while the production space and ecological space continue to shrink over the course of nearly 30 years of development. From the point of view of land use, the CCD of PLES in the Daqing River Basin peaked in 2010, after which conflicts between production space, living space, and ecological space gradually emerged. Under both NT and EP, the conflict between PLES in the Daqing River Basin will increase significantly in 2030 compared to 2020, while the CP scenario will mitigate the increase in conflict. PLES of the eastern, central, and western parts of the Daqing River Basin each have their own unique spatial evolutionary characteristics, and the changes of PLES in these three sub-regions are uneven. Enhancing cropland preservation is beneficial to the maintenance of the CCD of PLES in the central part, while enhancing ecological preservation is beneficial to the maintenance of the CCD in the east. Our findings complement the current understanding of the impact of land use change on PLES in a basin framework, highlight the heterogeneous nature of PLES change within basins, and deepen the understanding of the important role of cropland preservation in promoting sustainable regional development. In the formulation of land use policies, the Daqing River Basin needs to improve the use efficiency of the built-up land, avoid its indiscriminate expansion, minimize the occupation of cropland, and reduce the conflict between production functions and living functions. In addition, it is essential to pay more attention to the locality of land use, optimise the planting configuration of existing cropland, and strive to improve the productivity per unit area of it.

Author Contributions: Conceptualization, Q.L.; methodology, Q.L.; software, Q.L.; validation, Q.L. and D.Y.; formal analysis, Q.L.; investigation, Q.L.; resources, Q.L.; data curation, Q.L.; writing—original draft preparation, Q.L.; writing—review and editing, D.Y. and L.C.; visualization, Q.L.; supervision, D.Y. and L.C.; project administration, D.Y.; funding acquisition, D.Y. and L.C. All authors have read and agreed to the published version of the manuscript.

Funding: This research was funded by the National Natural Science Foundation of China (grant number 52078326) and Key Program of the National Natural Science Foundation of China (grant number 51838003).

Institutional Review Board Statement: Not applicable.

Informed Consent Statement: Not applicable.

Data Availability Statement: Not applicable.

Acknowledgments: The authors are grateful to the editor and reviewers for their valuable comments and suggestions.

Conflicts of Interest: The authors declare no conflict of interest.

References

- Chang, X.; Xing, Y.; Wang, J.; Yang, H.; Gong, W. Effects of Land Use and Cover Change (LUCC) on Terrestrial Carbon Stocks in China between 2000 and 2018. *Resour. Conserv. Recycl.* **2022**, *182*, 106333. [\[CrossRef\]](#)
- Lai, Z.; Chen, M.; Liu, T. Changes in and Prospects for Cultivated Land Use since the Reform and Opening up in China. *Land Use Policy* **2020**, *97*, 104781. [\[CrossRef\]](#)
- Liang, L.; Chen, M.; Luo, X.; Xian, Y. Changes Pattern in the Population and Economic Gravity Centers since the Reform and Opening up in China: The Widening Gaps between the South and North. *J. Clean. Prod.* **2021**, *310*, 127379. [\[CrossRef\]](#)
- Gonzalez-Gonzalez, A.; Clerici, N.; Quesada, B. A 30 m-Resolution Land Use-Land Cover Product for the Colombian Andes and Amazon Using Cloud-Computing. *Int. J. Appl. Earth Obs. Geoinf.* **2022**, *107*, 102688. [\[CrossRef\]](#)
- Cruz, J.D.S.; Blanco, C.J.C.; de Oliveira, J.F., Jr. Modeling of Land Use and Land Cover Change Dynamics for Future Projection of the Amazon Number Curve. *Sci. Total Environ.* **2022**, *811*, 152348. [\[CrossRef\]](#) [\[PubMed\]](#)
- Murillo-Sandoval, P.J.; Gjerdsseth, E.; Correa-Ayram, C.; Wrathall, D.; Van den Hoek, J.; Davalos, L.M.; Kennedy, R. No Peace for the Forest: Rapid, Widespread Land Changes in the Andes-Amazon Region Following the Colombian Civil War. *Glob. Environ. Chang.* **2021**, *69*, 102283. [\[CrossRef\]](#)
- Lidzhegu, Z.; Kabanda, T. Declining Land for Subsistence and Small-Scale Farming in South Africa: A Case Study of Thulamela Local Municipality. *Land Use Policy* **2022**, *119*, 106170. [\[CrossRef\]](#)
- Tulone, A.; Galati, A.; Pecoraro, S.; Carroccio, A.; Siggia, D.; Virzi, M.; Crescimanno, M. Main Intrinsic Factors Driving Land Grabbing in the African Countries' Agro-Food Industry. *Land Use Policy* **2022**, *120*, 106225. [\[CrossRef\]](#)
- Chen, Q.; Liu, Y.; Ge, Q.; Pan, T. Impacts of Historic Climate Variability and Land Use Change on Winter Wheat Climatic Productivity in the North China Plain during 1980–2010. *Land Use Policy* **2018**, *76*, 1–9. [\[CrossRef\]](#)
- Zhong, H.; Liu, Z.; Wang, J. Understanding Impacts of Cropland Pattern Dynamics on Grain Production in China: An Integrated Analysis by Fusing Statistical Data and Satellite-Observed Data. *J. Environ. Manag.* **2022**, *313*, 114988. [\[CrossRef\]](#)
- Liu, Q.; Yang, D.; Cao, L.; Anderson, B. Assessment and Prediction of Carbon Storage Based on Land Use/Land Cover Dynamics in the Tropics: A Case Study of Hainan Island, China. *Land* **2022**, *11*, 244. [\[CrossRef\]](#)
- Zhang, H.; Zhao, X.; Kang, M.; Han, J. Contrasting Changes in Fine-Scale Land Use Structure and Summertime Thermal Environment in Downtown Shanghai. *Sustain. Cities Soc.* **2022**, *83*, 103965. [\[CrossRef\]](#)
- Lu, Y.; Zhou, J.; Sun, L.; Gao, J.; Raza, S. Long-Term Land-Use Change from Cropland to Kiwifruit Orchard Increases Nitrogen Load to the Environment: A Substance Flow Analysis. *Agric. Ecosyst. Environ.* **2022**, *335*, 108013. [\[CrossRef\]](#)
- Chen, Z.; Li, Y.; Liu, Y.; Liu, X. Does Rural Residential Land Expansion Pattern Lead to Different Impacts on Eco-Environment? A Case Study of Loess Hilly and Gully Region, China. *Habitat Int.* **2021**, *117*, 102436. [\[CrossRef\]](#)
- Wang, Q.; Kang, Q.; Zhao, B.; Li, H.; Lu, H.; Liu, J.; Yan, C. Effect of Land-Use and Land-Cover Change on Mangrove Soil Carbon Fraction and Metal Pollution Risk in Zhangjiang Estuary, China. *Sci. Total Environ.* **2022**, *807*, 150973. [\[CrossRef\]](#) [\[PubMed\]](#)
- Feng, R.; Wang, F.; Wang, K.; Wang, H.; Li, L. Urban Ecological Land and Natural-Anthropogenic Environment Interactively Drive Surface Urban Heat Island: An Urban Agglomeration-Level Study in China. *Environ. Int.* **2021**, *157*, 106857. [\[CrossRef\]](#)
- Wang, A.; Liao, X.; Tong, Z.; Du, W.; Zhang, J.; Liu, X.; Liu, M. Spatial-Temporal Dynamic Evaluation of the Ecosystem Service Value from the Perspective of "Production-Living-Ecological" Spaces: A Case Study in Dongliao River Basin, China. *J. Clean. Prod.* **2022**, *333*, 130218. [\[CrossRef\]](#)
- Duan, Y.; Wang, H.; Huang, A.; Xu, Y.; Lu, L.; Jia, Z. Identification and Spatial-Temporal Evolution of Rural "Production-Living-Ecological" Space from the Perspective of Villagers' Behavior—A Case Study of Ertai Town, Zhangjiakou City. *Land Use Policy* **2021**, *106*, 105457. [\[CrossRef\]](#)
- Wu, J.; Zhang, D.; Wang, H.; Li, X. What Is the Future for Production-Living-Ecological Spaces in the Greater Bay Area? A Multi-Scenario Perspective Based on DEE. *Ecol. Indic.* **2021**, *131*, 108171. [\[CrossRef\]](#)
- Zou, L.; Liu, Y.; Wang, J.; Yang, Y. An Analysis of Land Use Conflict Potentials Based on Ecological-Production-Living Function in the Southeast Coastal Area of China. *Ecol. Indic.* **2021**, *122*, 107297. [\[CrossRef\]](#)
- Zhang, H.; Duan, Y.; Wang, H.; Han, Z.; Wang, H. An Empirical Analysis of Tourism Eco-Efficiency in Ecological Protection Priority Areas Based on the DPSIR-SBM Model: A Case Study of the Yellow River Basin, China. *Ecol. Inform.* **2022**, *70*, 101720. [\[CrossRef\]](#)
- Jin, M.; Weijermars, R. Economic Appraisal of an Unconventional Condensate Play Based on Public Pilot Data Prior to Field Development: Jafurah Basin Case Study (Saudi Arabia). *J. Nat. Gas Sci. Eng.* **2022**, *103*, 104605. [\[CrossRef\]](#)
- Zhou, M.; Deng, J.; Lin, Y.; Zhang, L.; He, S.; Yang, W. Evaluating Combined Effects of Socio-Economic Development and Ecological Conservation Policies on Sediment Retention Service in the Qiantang River Basin, China. *J. Clean. Prod.* **2021**, *286*, 124961. [\[CrossRef\]](#)
- Yang, Y.; Zhang, X.; Mu, Y.; Zhang, W. The Basic Logic and Core Strategies of Ecological Protection and High-Quality Development in the Upper Reaches of the Yellow River. *Econ. Geogr.* **2020**, *40*, 9–20.
- Han, H.; Guo, L.; Zhang, J.; Zhang, K.; Cui, N. Spatiotemporal Analysis of the Coordination of Economic Development, Resource Utilization, and Environmental Quality in the Beijing-Tianjin-Hebei Urban Agglomeration. *Ecol. Indic.* **2021**, *127*, 107724. [\[CrossRef\]](#)
- Hong, Y.; Liu, W.; Song, H. Spatial Econometric Analysis of Effect of New Economic Momentum on China's High-Quality Development. *Res. Int. Bus. Financ.* **2022**, *61*, 101621. [\[CrossRef\]](#)

27. Zhou, J.; Chen, Q.; Qi, P.; Liu, Z. Study on the Supply and Demand Matching for Policies Related to the Coordinated Development of High Haze Industries Such as Thermal Power Industry and Economy in the Beijing–Tianjin–Hebei Region. *Energy Rep.* **2022**, *8*, 502–512. [[CrossRef](#)]
28. Wang, Y. Analysis on the Evolution of Spatial Relationship between Population and Economy in the Beijing-Tianjin-Hebei and Shandong Region of China. *Sustain. Cities Soc.* **2022**, *83*, 103948. [[CrossRef](#)]
29. Deng, Y.; Yang, R. Influence Mechanism of Production-Living-Ecological Space Changes in the Urbanization Process of Guangdong Province, China. *Land* **2021**, *10*, 1357. [[CrossRef](#)]
30. Jiao, G.; Yang, X.; Huang, Z.; Zhang, X.; Lu, L. Evolution Characteristics and Possible Impact Factors for the Changing Pattern and Function of “Production-Living-Ecological” Space in Wuyuan County. *J. Nat. Resour.* **2021**, *36*, 1252–1267. [[CrossRef](#)]
31. Li, K.; Zhang, B.; Xiao, W.; Lu, Y. Land Use Transformation Based on Production–Living–Ecological Space and Associated Eco-Environment Effects: A Case Study in the Yangtze River Delta Urban Agglomeration. *Land* **2022**, *11*, 1076. [[CrossRef](#)]
32. Zou, Y.; Zhang, S.; Xie, Y.; Du, Y. Spatial Distribution and Evolution Characters of Production-Living-Ecological Spaces in Xuzhou City. *Sci. Surv. Mapp.* **2020**, *45*, 154–162.
33. Li, J.; Sun, W.; Li, M.; Meng, L. Coupling coordination degree of production, living and ecological spaces and its influencing factors in the Yellow River Basin. *J. Clean. Prod.* **2021**, *298*, 126803. [[CrossRef](#)]
34. Yang, Y.; Bao, W.; Liu, Y. Coupling Coordination Analysis of Rural Production-Living-Ecological Space in the Beijing-Tianjin-Hebei Region. *Ecol. Indic.* **2020**, *117*, 106512. [[CrossRef](#)]
35. Wei, L.; Zhang, Y.; Wang, L.; Mi, X.; Wu, X.; Cheng, Z. Spatiotemporal Evolution Patterns of “Production-Living-Ecological” Spaces and the Coordination Level and Optimization of the Functions in Jilin Province. *Sustainability* **2021**, *13*, 13192. [[CrossRef](#)]
36. Wang, C.; Tang, N. Spatio-Temporal Characteristics and Evolution of Rural Production-Living-Ecological Space Function Coupling Coordination in Chongqing Municipality. *Geogr. Res.* **2018**, *37*, 1100–1114.
37. Li, Q.; Su, Y.; Feng, Z.; Zhou, X.; Guo, L.; Ma, X.; Liu, G. Study on Production-Living-Ecological Space Function Coupling Coordination in Fen River Basin. *Sci. Soil Water Conserv.* **2021**, *19*, 115–125.
38. Li, Y.; Ye, C.; Huang, X. Temporal-Spatial Evolution and Scenario Simulation of Production-Living-Ecological Space in Nanchang Based on CLUE-S Model. *Res. Soil Water Conserv.* **2021**, *28*, 325–332.
39. Liu, X.; Liang, X.; Li, X.; Xu, X.; Ou, J.; Chen, Y.; Li, S.; Wang, S.; Pei, F. A Future Land Use Simulation Model (FLUS) for Simulating Multiple Land Use Scenarios by Coupling Human and Natural Effects. *Landsc. Urban Plan.* **2017**, *168*, 94–116. [[CrossRef](#)]
40. Liang, X.; Guan, Q.; Clarke, K.; Liu, S.; Wang, B.; Yao, Y. Understanding the Drivers of Sustainable Land Expansion Using a Patch-Generating Land Use Simulation (PLUS) Model: A Case Study in Wuhan, China. *Comput. Environ. Urban Syst.* **2021**, *85*, 101569. [[CrossRef](#)]
41. Zhang, S.; Zhong, Q.; Cheng, D.; Xu, C.; Chang, Y.; Lin, Y.; Li, B. Landscape Ecological Risk Projection Based on the PLUS Model under the Localized Shared Socioeconomic Pathways in the Fujian Delta Region. *Ecol. Indic.* **2022**, *136*, 108642. [[CrossRef](#)]
42. Wang, Z.; Li, X.; Mao, Y.; Li, L.; Wang, X.; Lin, Q. Dynamic Simulation of Land Use Change and Assessment of Carbon Storage Based on Climate Change Scenarios at the City Level: A Case Study of Bortala, China. *Ecol. Indic.* **2022**, *134*, 108499. [[CrossRef](#)]
43. Du, Y.; Li, X.; He, X.; Li, X.; Yang, G.; Li, D.; Xu, W.; Qiao, X.; Li, C.; Sui, L. Multi-Scenario Simulation and Trade-Off Analysis of Ecological Service Value in the Manas River Basin Based on Land Use Optimization in China. *Int. J. Environ. Res. Public Health* **2022**, *19*, 6216. [[CrossRef](#)] [[PubMed](#)]
44. Sun, T.; Cheng, W.; Bo, Q.; Meng, X.; Liang, D. Analysis on Historical Flood and Countermeasures in Prevention and Control of Flood in Daqing River Basin. *Environ. Res.* **2021**, *196*, 110895. [[CrossRef](#)]
45. Bo, Q.; Cheng, W.; Sun, T. Flow Capacity and Ice Cap Stability of River Channel in the Daqing River Basin of the South-to-North Water Diversion Project during the Ice Period. *Alex. Eng. J.* **2022**, *61*, 3657–3663. [[CrossRef](#)]
46. Gou, M.; Liu, C.; Li, L.; Xiao, W.; Wang, N.; Hu, J. Ecosystem Service Value Effects of the Three Gorges Reservoir Area Land Use Transformation under the Perspective of “Production-Living-Ecological” Space. *J. Appl. Ecol.* **2021**, *32*, 3933–3941.
47. Cui, J.; Gu, J.; Sun, J.; Luo, J. The Spatial Pattern and Evolution Characteristics of the Production, Living and Ecological Space in Hubei Province. *China Land Sci.* **2018**, *32*, 67–73.
48. Zhang, Y.; Luan, Q.; Xiong, C.; Liu, X. Spatial Heterogeneity Evaluation and Zoning of Production-Living-Ecological Space Based on Multi-source Spatial Data. *Trans. Chin. Soc. Agric. Eng.* **2021**, *37*, 214–223.
49. Cui, J.; Guo, G.; Zhang, H. Spatial Characteristics of Production-Living-Ecological Geographical Space of a Typical City in the Lower Yellow River Plain Area. *Yellow River* **2022**, *44*, 105–110.
50. Bai, R.; Jiang, Y.; Jiang, J. Multi-Scale Analysis on Functional Structure of Ecological-Production-Living Spaces of Jianghuai Urban Agglomeration. *China Anc. City* **2016**, *10*, 21–28.
51. Li, Y.; Li, Y.; Zhou, Y.; Shi, Y.; Zhu, X. Investigation of a Coupling Model of Coordination between Urbanization and the Environment. *J. Environ. Manag.* **2012**, *98*, 127–133. [[CrossRef](#)] [[PubMed](#)]
52. Yang, C.; Zeng, W.; Yang, X. Coupling Coordination Evaluation and Sustainable Development Pattern of Geo-Ecological Environment and Urbanization in Chongqing Municipality, China. *Sustain. Cities Soc.* **2020**, *61*, 102271. [[CrossRef](#)]
53. Yuan, J.; Bian, Z.; Yan, Q.; Pan, Y. Spatio-Temporal Distributions of the Land Use Efficiency Coupling Coordination Degree in Mining Cities of Western China. *Sustainability* **2019**, *11*, 5288. [[CrossRef](#)]
54. Ni, W. The Coupling and Coordination Relationship and Their Spatial Pattern of Urban Land Use Economic, Social and Ecological Benefits of Cities in Three Largest Urban Agglomerations in China. *Urban Dev. Stud.* **2016**, *23*, 69–77.

55. Ma, T.; Li, X.; Bai, J.; Ding, S.; Zhou, F.; Cui, B. Four Decades' Dynamics of Coastal Blue Carbon Storage Driven by Land Use/Land Cover Transformation under Natural and Anthropogenic Processes in the Yellow River Delta, China. *Sci. Total Environ.* **2019**, *655*, 741–750. [[CrossRef](#)] [[PubMed](#)]
56. Mansour, S.; Al-Belushi, M.; Al-Awadhi, T. Monitoring Land Use and Land Cover Changes in the Mountainous Cities of Oman Using GIS and CA-Markov Modelling Techniques. *Land Use Policy* **2020**, *91*, 104414. [[CrossRef](#)]
57. Zhang, Z.; Li, J. Spatial Suitability and Multi-Scenarios for Land Use: Simulation and Policy Insights from the Production-Living-Ecological Perspective. *Land Use Policy* **2022**, *119*, 106219. [[CrossRef](#)]
58. Liang, Y.; Hashimoto, S.; Liu, L. Integrated Assessment of Land-Use/Land-Cover Dynamics on Carbon Storage Services in the Loess Plateau of China from 1995 to 2050. *Ecol. Indic.* **2021**, *120*, 106939. [[CrossRef](#)]
59. Estoque, R.; Gomi, K.; Togawa, T. Scenario-Based Land Abandonment Projections: Method, Application and Implications. *Sci. Total Environ.* **2019**, *692*, 903–916. [[CrossRef](#)]
60. Dong, N.; You, L.; Cai, W.; Li, G.; Lin, H. Land Use Projections in China under Global Socioeconomic and Emission Scenarios: Utilizing a Scenario-Based Land-Use Change Assessment Framework. *Glob. Environ. Chang.* **2018**, *50*, 164–177. [[CrossRef](#)]
61. Sang, L.; Zhang, C.; Yang, J.; Zhu, D.; Yun, W. Simulation of Land Use Spatial Pattern of Towns and Villages Based on CA-Markov Model. *Math. Comput. Model.* **2011**, *54*, 938–943. [[CrossRef](#)]
62. Hoque, M.; Cui, S.; Islam, I.; Xu, L.; Ding, S. Dynamics of Plantation Forest Development and Ecosystem Carbon Storage Change in Coastal Bangladesh. *Ecol. Indic.* **2021**, *130*, 107954. [[CrossRef](#)]
63. Huang, D.; Dong, W.; Wang, Q. Spatial and Temporal Analysis of Human Infection with the Avian Influenza A (H7N9) Virus in China and Research on a Risk Assessment Agent-Based Model. *Int. J. Infect. Dis.* **2021**, *106*, 386–394. [[CrossRef](#)] [[PubMed](#)]
64. Ni, Y.; Wang, M. The Characteristics and Influencing Factors of Geographical Agglomeration of Forage Industry in China. *Econ. Geogr.* **2018**, *38*, 142–150.
65. Yang, Q.; Liu, Q.; Yin, S.; Zhang, J.; Yang, X.; Gao, Y. Vulnerability and Influencing Factors of Rural Transportation Environment in Qinling-Daba Mountainous Areas: A Case Study of Luonan County in Shaanxi Province. *Acta Geogr. Sin.* **2019**, *74*, 1236–1251.
66. Bao, W.; Yang, Y.; Zou, L. How to Reconcile Land Use Conflicts in Mega Urban Agglomeration? A Scenario-Based Study in the Beijing-Tianjin-Hebei Region, China. *J. Environ. Manag.* **2021**, *296*, 113168. [[CrossRef](#)]
67. Rong, Y.; Du, P.; Sun, F.; Zeng, S. Quantitative Analysis of Economic and Environmental Benefits for Land Fallowing Policy in the Beijing-Tianjin-Hebei Region. *J. Environ. Manag.* **2021**, *286*, 112234. [[CrossRef](#)]
68. Luo, Y.; Zhou, D.; Tian, Y.; Jiang, G. Spatial and Temporal Characteristics of Different Types of Pollution-Intensive Industries in the Beijing-Tianjin-Hebei Region in China by Using Land Use Data. *J. Clean. Prod.* **2021**, *329*, 129601. [[CrossRef](#)]
69. Jiang, X.; Zhai, S.; Liu, H.; Chen, J.; Zhu, Y.; Wang, Z. Multi-Scenario Simulation of Production-Living-Ecological Space and Ecological Effects Based on Shared Socioeconomic Pathways in Zhengzhou, China. *Ecol. Indic.* **2022**, *137*, 108750. [[CrossRef](#)]
70. Zhong, S.; Wang, M.; Zhu, Y.; Chen, Z.; Huang, X. Urban Expansion and the Urban-Rural Income Gap: Empirical Evidence from China. *Cities* **2022**, *129*, 103831. [[CrossRef](#)]
71. Min, M.; Duan, X.; Yan, W.; Miao, C. Quantitative Simulation of the Relationships between Cultivated Land-Use Patterns and Non-Point Source Pollutant Loads at a Township Scale in Chaohu Lake Basin, China. *CATENA* **2022**, *208*, 105776. [[CrossRef](#)]